Journal of the Korean Magnetic Resonance Society **2004**, *8*, 19 - 27

Structure of CT16 in the C-terminal of Amyloid Precursor Protein Studied by NMR Spectroscopy

Kyoungik Lee, Dongha Baek, Song Yub Shin[1] and Yangmee Kim*

Department of Chemistry, Konkuk University, Seoul 143-701, Korea
[1]Department of Bio-Materials, Graduate School and Research Center for Proteineous Materials, Chosun University, Gwangju 501-759, Korea
Received March 10, 2004

Abstract : C-terminal fragments of APP (APP-CTs), that contain complete Abeta sequence, are found in neuritic plaques, neurofibrillary tangles and the cytosol of lymphoblastoid cells obtained from AD patients. CT16, Lys649-Asp664 (KKQYTSIHHGVVEVD) has been known as the most toxic part in the C-terminal fragment of amyloid precursor protein (APP). The solution structure of CT16 was investigated using NMR spectroscopy in various membrane-mimicking environments. According to Circular Dichroim (CD) spectra, CT16 has a random structure in aqueous solution, while conformational change was induced by addition of TFE and SDS micelle. Tertiary structure as determined by NMR spectroscopy shows that CT16 has a β -turn conformation in trifluoroethanol-containing aqueous solution.

INTRODUCTION

Alzheimer's disease (AD) is the most common causative brain disease of primary dementia in the elderly. The most characteristic change in progressive dementia of Alzheimer's type is a tissue deposit of amyloid beta peptide, which is derived from its precursor protein APP.[1-11] Mutations in the beta-amyloid precursor protein (APP) gene cause familial Alzheimer's disease (AD). Although amyloid beta peptide (Abeta) is the principal constituent of senile plaques in AD, other cleavage products of APP are also implicated in playing a role in the pathogenesis of AD. C-terminal fragments of APP (APP-

* To whom correspondence should be addressed. E-mail: keysun@kist.re.kr

CTs), that contain complete Abeta sequence, are found in neuritic plaques, neurofibrillary tangles and the cytosol of lymphoblastoid cells obtained from AD patients. Structural alteration of APP are implicated in the pathogenesis of Alzheimer's disease, but it is not known how they cause the disease.[1-11] The amyloid precursor protein presents several cleavage sites leading to the release of its entire C-terminal domain into the cytoplasm. During apoptosis, this C-terminal domain can be cleaved at amino acid 664 by caspases 3, 6 and 8 and can thus generate two peptides N- and C-terminal to amino acid 664 (C31). Recently, it was shown that the C31 induces apoptosis after transfection into N2A and 293 T cell lines.[12] It has been found that whereas micromolar concentrations of APP-Cter are harmless, the peptide extending from the membrane (amino acid 649) to the caspase cleavage site (amino acid 664) in the same range of concentrations induces DNA fragmentation, cleavage of actin at a caspase-sensitive site, and activates caspase 3. A mutated version of this sequence (tyrosine 653 replaced by an aspartate) abolishes the effect in vitro and in vivo. This APP sequence, Lys649-Asp664 (CT16, KKQYTSIHHGVVEVD) contributs to Alzheimer's Disease-associated cell death and the most toxic part in the C-terminal of APP. [12-14]

In order to understand the conformational basis of the pathological activity of the C-terminal fragments of APP, the structure of CT16 has been studied. Here, we determined the three-dimensional structures of CT16 using CD and NMR spectroscopy in membrane mimetic environments.

EXPERIMENTALS

Sample preparation.

Peptides were synthesized on Rink Amide MBHA resin as C-terminal amides by the solid phase method using Fmoc-chemistry, and were purified by a preparative reverse-phase C_{18} column. Trifluoroethanol (TFE) was purchased from ALDRICH Chemical Co. and perdeuterated sodium dodecyl sulfate (SDS-d_{25}) was obtained from Cambridge Isotope Inc. For NMR experiments in SDS micelle, peptide was dissolved in 0.45mL of 120mM SDS micelle to make a final concentration of 2.0 mM.

CD Experiments

CD measurements of 100 μM peptide solutions were performed on a J720 spectropolarimeter (Japan, Jasco) between 190 and 250 nm at 25°C. In order to investigate the conformations in membrane-like environment, peptides were dissolved in 30%-70% (v/v) TFE-containing aqueous solution and SDS micelles, and DPC micelles.

NMR spectroscopy

All of the NMR experiments for the sample in SDS micelle were performed at 298K. All the phase sensitive two-dimensional experiments such as DQF-COSY [15], TOCSY [16], and NOESY[17] experiments were performed using time-proportional phase incrementation(TPPI) method. [18,19] For these experiments, 400-512 transients with 2K complex data points were collected for each of the increments with a relaxation delay of 1.2-1.5 sec between the successive transients and the data along the t_1 dimension were zerofilled to 1K before 2D-Fourier transformation. TOCSY experiment was performed with mixing times of 80-100 msec, MLEV-17 spin-lock mixing pulse. NOESY experiments were performed with mixing times of 150 and 250 msec.

All NMR spectra were recorded on Bruker DPX-400 spectrometer in Konkuk University. All NMR spectra were processed off-line using the FELIX software package (Molecular Simulations Inc., San Diego) on SGI workstation in our laboratory.

Chemical shifts of the samples were measured relative to the methyl resonance of internal 2,2-dimethyl-2-silapentane-5-sulfonic acid(DSS) at 0 ppm. $^3J_{HN\alpha}$ coupling constants were either measured in 1D spectrum or calculated from the separation of absorptive peaks and dispersive peaks in DQF-COSY spectrum. DQF-COSY spectrum was processed to the 4K×2K matrix and used to measure peak-to-peak separations. P.E.COSY experiment was executed to obtain $^3J_{\alpha\beta}$ coupling constants. To identify slowly exchanging amide protons, a series of 1D spectra were acquired after deuterium oxide was added to the sample.

Structure calculation.

Structure calculations were carried out using X-PLOR version 3.851.[20] All the NOE intensities are divided into three classes, i.e., strong, medium, and weak with the distance ranges of 1.8-2.7, 1.8-3.5, and 1.8-5.0Å, respectively. [21,22] Standard pseudoatom

corrections were applied to the non-stereospecifically assigned restraints,[23] and the additional 0.5 Å was added to the upper bounds for NOEs involving methyl protons. [24] Standard distance geometry-dynamical simulated annealing hybrid protocol[25,26] was imployed to generate structures. Center averaging was used to correct distances involving methyl groups and non-stereospecifically assigned methylene. The target function that is minimized during simulated annealing comprises only quadratic harmonic potential terms for covalent geometry, square-well quadratic potentials for the experimental distance and torsion angle restraints, and a quartic van der Waals repulsion term for the nonbonded contacts.

RESULTS and DISCUSSION

Fig. 1 shows the CD spectrum of CT16 in water, TFE/water solution (v/v), SDS micelles and DPC micelles. CT16 has a random coil structure in water. Addition of TFE induced structural changes, but CT16 in SDS micelles and DPC micelles do not show big difference from one in aqueous solution. In order to investigate the tertiary structure of CT16 and understand the structural changes induced by TFE, we determined the tertiary structure of TFE/water solution using NMR spectroscopy.

Using standard sequential assignment strategy[27], all the proton resonances were assigned. TOCSY and DQF-COSY spectra were used to assign spin systems of most of the amino acid residues. By direct comparison of TOCSY and NOESY spectra, sequence-specific resonance assignments were completed. Table 1 lists the complete assignments of the proton chemical shifts of CT16 in TFE/water solution 277K. The sequential NOE connectivities in the fingerprint region of NOESY spectra of CT16 in SDS micelle are illustrated in Fig. 2.

Fig. 3 illustrates the summary of the NOE connectivities of CT16 in TFE/H_2O(1:1, v/v) solution, which were extracted directly from NOESY spectrum recorded with a mixing time of 250msec. Medium-range, i.e., *i*-*i*+2 NOE connectivities are observed from Thr6-Ile8 and from His9 to Gly11. Total of 50 structures were generated by hybrid distance geometry-dynamical simulated annealing algorithm, and 20 structures having lowest energies were selected for further analysis.

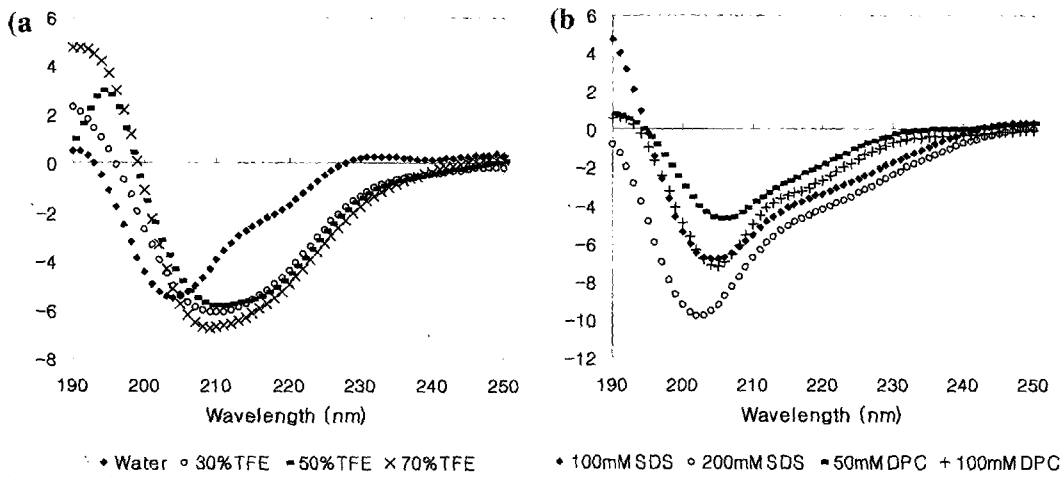

Fig. 1. Circular Dichroism spectra of CT16 in various environments. (a) in TFE-H_2O mixture solvents (b) in sodium dodecylsulfate (SDS) micelles and dodecylphosphocholine (DPC) micelles.

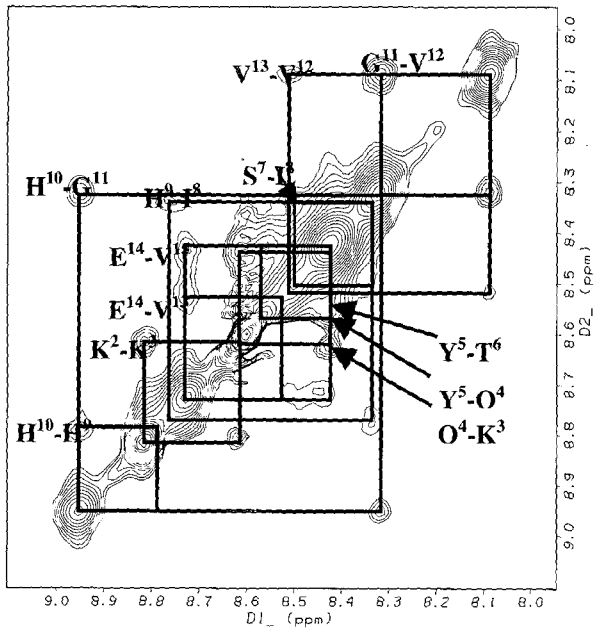

Fig. 2. The NH-N region of a NOESY spectrum of CT16 with a mixing time of 250 msec in TFE/water solution at 277K, pH 4.0.

Table 1. ^{1}H chemical shifts (ppm) for CT16 in TFE/H_2O(1:1, v/v) solution at 277K, pH 4.0

Residue	*Chemical shift(ppm)*[a]				$^3J_{HN\alpha H}$
	NH	αH	βH	Others	
Lys[1]					
Lys[2]	8.81	4.41	1.86*	γ 1.49*; δ 1.74*; ε 3.00*	8
Lys[3]	8.61	4.33	1.76*	γ 1.39, 1.45; δ 1.70*; ε 3.08*	8
Gln[4]	8.42	4.58	1.93, 2.02	γ 2.31*	8
Tyr[5]	8.53	4.36	2.92, 3.08	2, 6H 7.13; 3, 5H 6.86	8
Thr[6]	8.42	4.72	4.11	γ 1.18*	8
Ser[7]	8.47	4.36	3.88*		8
Ile[8]	8.33	4.40	1.76	γ CH_3 0.91*; γ CH_2 1.08*; δ 0.84*	8
His[9]	8.74	4.67	3.13, 3.24	2H 8.59; 4H 7.23	9
His[10]	8.95	4.46	3.26, 3.40	2H 8.60; 4H 7.29	6
Gly[11]	8.31	3.91, 4.06			
Val[12]	8.08	4.37	2.14	γ 0.99*	9
Val[13]	8.50	4.34	2.03	γ 0.92*	8
Glu[14]	8.71	4.66	1.94, 2.07	γ 2.37*	8
Val[15]	8.43	4.48	2.05	γ 0.93*	8
Asp[16]	8.40	4.66	2.80, 2.89		8

[a]*Chemical shifts are relative to DSS(0 ppm).*

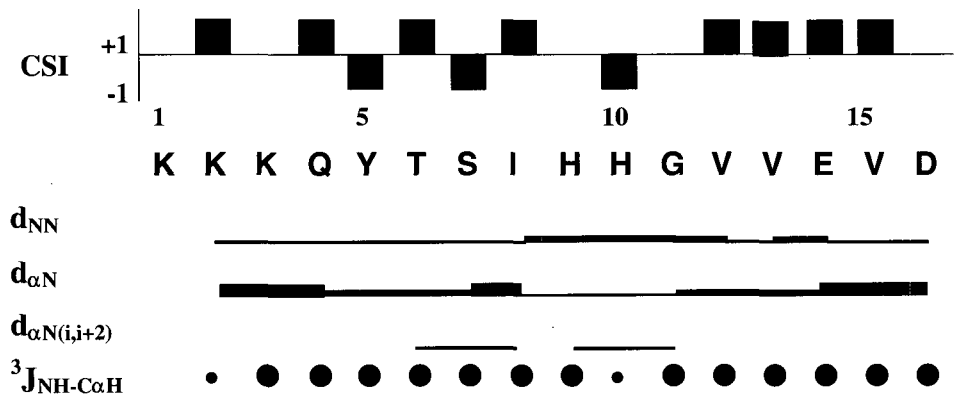

Fig. 3. The NOE connectivities, $^3J_{HN\alpha}$ coupling constants and chemical shift index of CT16 in TFE/H_2O(1:1, v/v) solution at 277K, pH 4.0. The size of filled circle is proportional to the value of measured $^3J_{NH\text{-}C\alpha H}$.

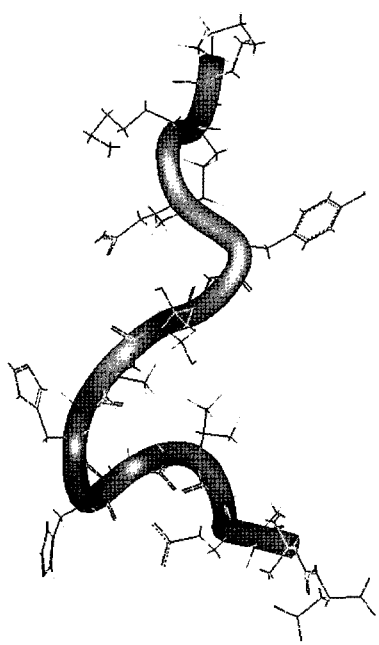

Fig. 4. Lowest energy structure of CT16 in TFE/water solution. Ribbon diagrams for the backbones and the all atoms are displayed here.

All of structures satisfies the experimental NOEs well within 0.02Å. All structures display good covalent geometry and small NMR constraint violations. The mean structure was obtained by restrained minimization of the averaged coordinates of the 20 final structures of each peptide. However, all the structures have big flexibilities and show high rmsd between the structures when it was overlayed over the backbone heavy atoms of the mean structure. These high rmsd values might come from the lack of NOEs for CT16.

Fig. 4 shows the ribbon structure of the lowest energy structure of CT16 with all atoms The imidazole rings of two histidines protrude outside of turn structure. Overall structure does not have specific secondary structure except β-turn in the middle. It may have more defined structure upon binding to the specific receptor when it shows the neurotoxicity. Further structural studies on CT26 which includes the CT16, and the CT31 at the C-terminus of amyloid precursor proteins are on going in our laboratory. This preliminary study may help to give some insight to understand the conformational basis of the pathological activity of the C-terminal fragments of APP.

Acknowledgments

This study was supported by grants from the Ministry of Science and Technology, Korea, and from the Korea Science and Engineering Foundation through the Research Center for Proteineous Materials.

REFERENCES

1. Y. H. Suh, *Life Science & Biotechnology* 14, 16-19 (2000).
2. D. J. Selkoe, *J. Neuropathol. Exp. Neurol.* 53, 438-447 (1994).
3. F. Checler, *J. Neurochem.* 65, 1431-1444 (1995).
4. C. Haass, E. H. Koo, A. Mellon, A. Y. Hung and D. J. Selkoe, *Nature* 357, 500-503 (1992).
5. T. E. Golde, S. Estus, L. H. Younkin, D. J. Selkoe and and S. G. Younkin, *Science* 255, 728-730 (1992).
6. A. Matsumoto, *Biochem. Biophys. Res. Commun.* 175, 361-365 (1994).
7. F. Kametani, K. Tanaka, T. Tokuda and S. Ikeda, *FEBS Lett.* 351, 165-167 (1994).
8. T. Dyrks, E. Dyrks, T. Hartmann, C. Masters and K. Beyruther, *J. Biol. Chem.* 267, 18210-18217 (1992).
9. K. Fukuchi, B. Sopher, C. E. Furlong, J. A. Sundstrom, A. C. Smith and G. M. Martin, *Neurosci. Lett.* 154, 145-148 (1993).
10. M. L. Oster-Granite, J. Greenan and R. L. Neve, *J. Neurosci.* 16, 6732-6741 (1996).
11. J. Arters, D. Mcphie, R. L. Neve and J. Berger-Sweeny, *Soc. Neurosci. Abst.* 21, 1483 (1995).
12. E. Bertrand, E. Brouillet, I. Caille, C. Bouillot, G. M. Cole, A. Prochiantz, and B. Allinquant, Mol Cell Neurosci. 18(5), 503-11 (2001).
13. J. P. Lee, K. A. Chang, H. S. Kim, S. S. Kim, S. J. Jeong and Y. H. Suh, *J. Neurosci. Res.* 60, 565-570 (2000).
14. L. Albert, S. Sangram, Sisodia and S. T. Ian, *J. Biol. Chem.* 270, 3565-3573 (1995).
15. A. Derome and M. Willamson, *J. Magn. Reson.* 88, 177 (1990).
16. A. Bax and D. G. Davis, *J. Magn. Reson.* 65, 355 (1985).
17. S. Macura and R.R. Ernst, *Mol. Phys.* 41, 95 (1980).

18. A. Bax and D. G. Davis, *J. Magn. Reson.* 63, 207 (1985).
19. G. Bodenhausen and D. J. Ruben, *J. Chem. Phys. Lett.* 69, 185 (1980).
20. A. T. Brünger, *X-PLOR Manual, Version 3.1*, Yale University, New Haven, CT (1993).
21. G. M. Clore and A. M. Gronenborn, *CRC. Rev. in Biochem. Biol.* 24, 479 (1989).
22. G. M. Clore and A. M. Gronenborn, *Protein Science* 3, 372 (1994).
23. K. Wüthrich , M. Billeter, and W. Braun, *J. Mol. Biol.* 169, 949-961, (1983).
24. G. M. Clore, A. M. Gronenborn, M. Nilges, and C. A. Ryan, *Biochemistry* 26, 8012-8023 (1987).
25. M. Nilges, G. M. Clore, and A.M. Gronenborn, *FEBS Lett.* 229, 317-324 (1988).
26. J. Kuszewski, M. Nilges, and A. T. Brünger, *J. Biomol. NMR* 2, 33-56 (1992).
27. K. Wuthrich, in *"NMR of Protein and Nuclieic acid"*, Wiley, New York, (1986).